Experimental characterization of phase tuning using fine wavelength offsets in a tunable complex-coefficient optical tapped-delay-line

Salman Khaleghi,[1,*] Mohammad Reza Chitgarha,[1] Omer F. Yilmaz,[1] Moshe Tur,[2] Michael W. Haney,[3] Carsten Langrock,[4] Martin M. Fejer,[4] and Alan E. Willner[1]

[1]*Department of Electrical Engineering, University of Southern California, Los Angeles, California 90089, USA*

[2]*School of Electrical Engineering, Tel Aviv University, Ramat Aviv 69978, Israel*

[3]*Department of Electrical and Computer Engineering, University of Delaware, Newark, Delaware 19716, USA*

[4]*Edward L. Ginzton Laboratory, Stanford University, Stanford, California 94305, USA*

**Corresponding author: khaleghi@usc.edu*

Received September 30, 2013; revised December 27, 2013; accepted December 31, 2013; posted January 3, 2014 (Doc. ID 198309); published February 3, 2014

We use fine-detuning of pump wavelengths to adjust the tap phases in a complex-coefficient optical tapped-delay-line that utilizes conversion/dispersion-based delays and nonlinear wave mixing. Full 2π phase tuning is demonstrated by detuning the frequency of laser pumps by <20 GHz, which shows close agreement with theory.

OCIS codes: (060.2360) Fiber optics links and subsystems; (060.4370) Nonlinear optics, fibers; (190.4223) Nonlinear wave mixing.

http://dx.doi.org/10.1364/OL.39.000735

Tapped-delay-lines (TDLs) are key building blocks for various analog and digital signal processing applications, including finite impulse response (FIR) filtering, waveform generation, correlation, equalization, and discrete Fourier-transform [1,2]. In a TDL, the incoming signal is tapped at different time intervals; each tap is multiplied by a complex (amplitude and phase) coefficient, and taps are then added together. Optical implementations of TDLs have been of interest for many years [3–5]. Because tunable filters can provide more functions than static filters, it may be useful to develop optical TDL schemes that allow for continuous tunability of the TDL parameters to accommodate different applications [2].

Recent work on optical TDL systems has investigated fixed fiber-based structures [3], cascaded Mach–Zehnder interferometers [4–6], and opto-electronic approaches that utilize microwave techniques [7]. In general, these optical approaches tend to be either fixed or partially tunable over a finite range for some parameters.

Recently [2], we experimentally demonstrated a fully tunable complex-coefficient optical TDL (FIR filter) based on conversion/dispersion delays in which all crucial parameters of the TDL (number of taps, tap delays, tap amplitudes, tap phases) could be changed by varying the properties of the tunable pump lasers that were injected into the system [2]. The system utilized nonlinear wavelength multicasting, conversion–dispersion tunable delays, and nonlinear multiplexing to achieve tunability and reconfigurability. With this technique, the tap amplitudes and delays can be independently determined by the power and wavelength of the pump lasers, respectively. In our previous demonstrations, [2], a phase programmable filter (based on spatial light modulation) was required to set the tap phases. This implementation, however, may not be appropriate for integration purposes.

In this Letter, we theoretically derive and experimentally characterize an alternative technique for adjustment of the tap phases, using fine frequency detuning of the pump lasers. While propagating through the delay-generating dispersion elements in our system, the proposed frequency detuning is converted to the required tap phases. Our results demonstrate the continuous 2π tunability of phases with a laser frequency detuning of <20 GHz, with negligible error on the wavelength-dependent tap delays. The amount of fine-detuning required depends on the dispersion parameter and the difference between the pump wavelengths [8].

Figure 1 illustrates the principle of operation of our tunable optical TDL. First, cascaded second order $\chi^{(2)}$ nonlinear processes of sum frequency generation (SFG), followed by difference frequency generation (DFG), are exploited in a periodically poled lithium niobate (PPLN) device with the aid of multiple tunable dummy pump lasers to multicast the signal to N copies at different frequencies. The cascaded $\chi^{(2)}$ processes of SFG–DFG in a PPLN device resemble the $\chi^{(3)}$ process of four-wave-mixing (FWM) in highly nonlinear fibers [9,10]. The signal at frequency ω_{signal}, and a continuous wave (CW) pump at ω_{P1}, symmetrically located around the quasi-phase matching (QPM) frequency ω_{QPM} of the PPLN waveguide, mix through the SFG nonlinear process and the resulting signal then mixes with dummy pumps at ω_{Di} through the DFG process. These cascaded mixings create signal copies at frequencies $\omega_{\text{Ci}} = \omega_{\text{signal\_in}} + \omega_{P1} - \omega_{\text{Di}}$. Subsequently, these replicas travel through a chromatic dispersive element (e.g., a dispersion compensating fiber (DCF) of length L and group velocity dispersion parameter β_2) at different speeds, incurring a distinct time delay with respect to the first copy $T_i \approx L\beta_2(\omega_{\text{Di}} - \omega_{D1})$ [11]. Finally, these N replicas and their dummy pumps are sent into the second PPLN device together with another CW pump at ω_{P2} to be multiplexed using the cascaded SFG–DFG processes, resulting in a multiplexed output signal at frequency $\omega_{\text{signal\_out}} = \omega_{\text{Di}} + \omega_{\text{Ci}} - \omega_{P2} = \omega_{\text{signal\_in}} + (\omega_{P1} - \omega_{P2})$. As discussed in [2], the multiplexed output signal is proportional to

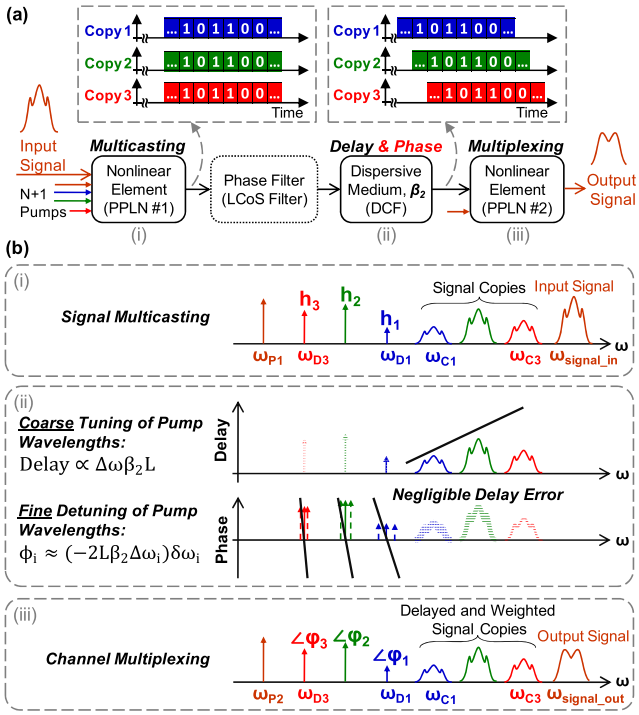

Fig. 1. Principle of operation of a complex-coefficient optical TDL, having three taps in (a) block diagram and (b) schematic spectrum of the three main stages: (i) the input signal is multicast to multiple copies where the wavelengths of the new copies and their powers are determined by the wavelengths and powers of the ω_{Di} dummy pumps that create them independently; (ii) dispersive medium induces delays between the signal copies by coarse-tuning of ω_{Di} pump wavelengths and enables adjusting the tap phases by fine-detuning of ω_{Di} pumps; and (iii) multiplexing the weighted and delayed copies to a single channel to form the output signal.

$$E_{\mathrm{signal\_out}}(t) \propto E_{P2}^{*} E_{P1} \sum_{i=1}^{N} (E_{\mathrm{Di}}^{*} E_{\mathrm{Di}}) e^{j(\Phi_i + \phi_i^{\mathrm{ADJ}})} E_{\mathrm{signal\_in}}(t - T_i), \tag{1}$$

in which $E_{\mathrm{signal\_in}}(t)$ is the electric field of the input optical signal and $E_{\mathrm{signal\_out}}(t)$ is the electric field of the output of the TDL. E_{P1} and E_{P2} denote the electric field amplitudes of the CW pumps at ω_{P1} and ω_{P2}, respectively, which uniformly affect all copies (taps). The asterisks denote complex conjugation. The products $E_{\mathrm{Di}}E_{\mathrm{Di}}^{*}$, which are proportional to the powers of the dummy pumps, serve here as the amplitudes of the FIR filter taps. The phase of each tap is mainly determined by the chromatic dispersion experienced by ω_{Di}, namely, [2]:

$$\begin{aligned} \Phi_i &= -2 \sum_{n=0}^{\infty} \frac{(\omega_{\mathrm{Di}} - \omega_{\mathrm{QPM}})^{2n}}{(2n)!} L\beta_{2n} \\ &= -2L\beta_0 - (\omega_{\mathrm{Di}} - \omega_{\mathrm{QPM}})^2 L\beta_2 - \ldots, \end{aligned} \tag{2}$$

in which $\beta_k = \partial^k \beta / \partial \omega^k |_{\omega=\omega_{\mathrm{QPM}}}$ is the kth derivative of the wave's propagation parameter $\beta(\omega)$ calculated at angular frequency ω_{QPM}. We note that because of the symmetry of ω_{Di}'s and ω_{Ci}'s around the QPM frequency, only the even terms remain in the Taylor series expansion in Eq. (2). To achieve the required tap phase, Φ_i should be augmented by an adjustable component ϕ_i^{ADJ}. Thus, the relationship between the input and output of the system can be written in the form of a complex-coefficient FIR filter as

$$E_{\mathrm{signal\_out}}(t) \propto \sum_{i=1}^{N} |h_i| e^{j\angle h_i} E_{\mathrm{signal\_in}}(t - T_i), \tag{3}$$

in which h_i is the complex weight of the i-th delayed copy. Its amplitude is the power of the i-th dummy pump ω_{Di} and its phase is related to the physical parameters of the system according to $\angle h_i = (\Phi_i + \phi_i^{\mathrm{ADJ}})$. In [2], a phase programmable liquid crystal on silicon (LCoS) filter was used to adjust ϕ_i^{ADJ}. This LCoS can now be omitted if, instead, the same phase adjustment is obtained by a fine-detune of the ω_{Di} pump frequencies. Indeed, if ω_{Di} is detuned by $\delta\omega_{\mathrm{Di}}$ and when ω_{Ci} and ω_{Di} are symmetrically located around ω_{QPM}, the tap phase changes by

$$\phi_i^{\mathrm{ADJ}} = \delta\Phi_i \approx -2L\beta_2(\omega_{\mathrm{Di}} - \omega_{\mathrm{QPM}})\delta\omega_{\mathrm{Di}}, \tag{4}$$

where the contribution of higher order even terms (e.g., β_4) will be experimentally confirmed to be negligible. Unavoidably, this $\delta\omega_{\mathrm{Di}}$ will also affect the delay through

$$\delta T_i / T_i \approx \delta\omega_{\mathrm{Di}} / (\omega_{\mathrm{Di}} - \omega_{D1}). \tag{5}$$

We studied this trade-off and determined that, for pumps reasonably far from each other and/or ω_{QPM}, this delay error can be practically ignored.

In summary, tap delays for the required FIR filtering are set by coarse-tuning of the pump wavelengths; the amplitudes of the tap weights are determined by the pump powers and their phases are adjusted by fine-detuning of the pump wavelengths. Finally, the number of taps can be scaled by using more dummy lasers. Because more taps occupy more bandwidth, the increase in the number of taps is eventually limited by the bandwidth of the components in use and their maximum power tolerance. The PPLN used can provide >70 nm conversion bandwidth for multicasting using SFG–DFG [9]. The requirement of tunable pumps adds to the system complexity; however, tunable pumps can enable a wide range of tuning for tap delays, which may be difficult to achieve with alternative approaches [3–6].

Figure 2(a) shows the experimental setup for the characterization of the detuning-induced phase adjustment. A CW input signal at wavelength $\lambda_{\mathrm{signal}} \approx 1540.8$ nm, a pump at $\lambda_{P1} \approx 1559.2$ nm, and a dummy pump at $\lambda_{D1} \approx 1549.5$ nm combined with another tunable (for different delays) dummy λ_{D2} (at ~1552.2 nm, ~1554.1 nm, ~1555.9 nm, or ~1557.7 nm) are separately amplified, filtered, and launched into the first 4-cm-long PPLN waveguide for multicasting. The output spectrum of PPLN 1 is shown in Fig. 2(b). For the calibration of the proposed detuning-induced phase adjustment, the output is also sent into an already calibrated amplitude and phase programmable LCoS filter that (i) passes the signal copies and dummy pumps, but blocks the original signal and λ_{P1} pump and (ii) is used to measure (with 5° accuracy) and validate the amount of phase shift created by the detuning. Subsequently, the copies and pumps pass through either a spool of ~170 m or ~450 m DCF with a dispersion parameter of $-2\pi c\beta_2/\lambda^2 = -80$ ps/nm/km. These two DCF spools allow for experiments with a total

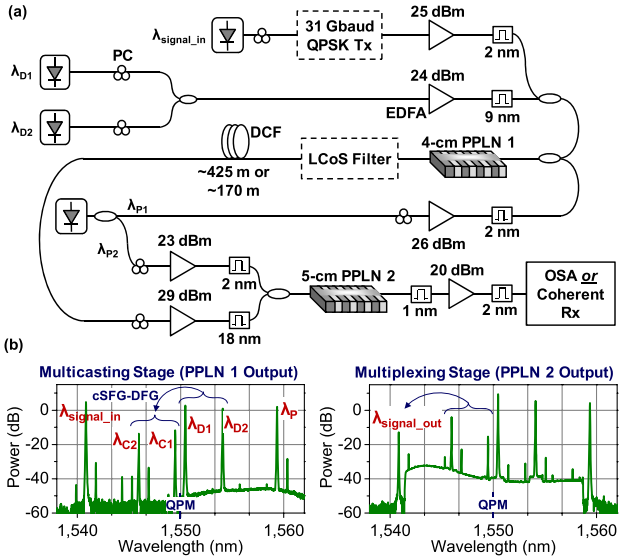

Fig. 2. (a) Experimental setup for the tunable optical TDL using optical multicasting, conversion/dispersion delays, and optical multiplexing. (b) Output spectra of PPLN 1 and PPLN 2.

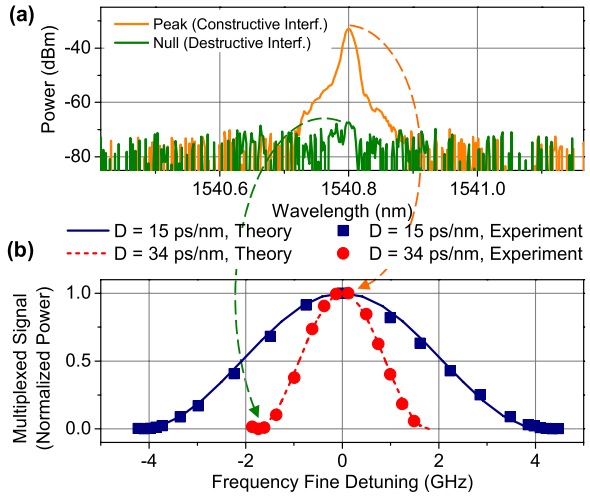

Fig. 3. (a) Constructive or destructive interference could create a peak or a null at the output, used for phase characterization. (b) Interference fringes caused by fine-detuning of pump frequencies for different amounts of dispersion.

dispersion of 15 ps/nm or 34 ps/nm. Next, the signals are amplified, filtered, combined with a CW pump λ_{P2}, and sent to the second 5-cm-long PPLN waveguide. Amplified signals and pumps are filtered before the PPLNs to eliminate the residual EDFA noise and wave mixing parasitic terms at the frequencies of the generated output signals. The QPM wavelengths of the two PPLN waveguides are thermally tuned to ~1550 nm. The λ_{P1} pump is split and used as λ_{P2} as well; therefore, the multiplexed output signal lands on the original signal frequency [Fig. 2(b), PPLN 2 output spectrum]. The output signal is finally filtered and sent to an optical spectrum analyzer (OSA) for power measurements. Later in the Letter, and to further assess the performance of the system, the CW signal is modulated using an IQ modulator to generate a quadrature-phase-shift-keyed (QPSK) signal at the 31 Gbaud data rate (pseudorandom bit sequence of length $2^{31}-1$) and detected using a coherent optical receiver.

Because only two taps are used to study the phase tuning characteristics, the output has the form of $y(t) = x(t) + |h_0|e^{j\angle h_0}x(t-T)$, which can result in constructive or destructive interference depending on the value of $\angle h_0 = \phi_i^{\mathrm{ADJ}}$. The amplitude of the tap is set to $|h_0| = 1$ by choosing appropriate powers for the dummy lasers. The value of ϕ_i^{ADJ} can be adjusted in this setup by wavelength detuning or the LCoS filter, or both, where the LCoS filter can negate and cancel the effect of the detuning, thereby also measuring it.

Figure 3(a) shows the multiplexed signal for the two cases of constructive and destructive interference, creating a peak or a null with a >35 dB extinction ratio. In Fig. 3(b), the wavelength of λ_{D2} (located 4.1 nm from λ_{QPM}) is finely detuned and the power is measured for two dispersion values. The resulting squared-cosine-shape fringes closely match theory derived in Eq. (4), and one can see that higher dispersion would require finer tuning.

Figure 4(a) shows the theoretical and experimentally measured phases induced by fine-detuning the tap wavelengths. As predicted in Eq. (4), the slope of the phase change versus frequency depends on the separation between the wavelength of the pump and that of the QPM. Taps with a longer time delay require larger pump–QPM wavelength separation and require less fine-detuning. Figure 4(b) illustrates fine-detuning of the CW pump located 4.2 nm away from the QPM wavelength [i.e., solid line in Fig. 4(a)].

In Fig. 5, the amount of frequency detuning required for a 360° phase shift is plotted versus the relative location of the tap (i.e., tap delay) for different dispersion values. Once again, theory and experiments are in agreement, proving that the longer delays and larger dispersions require less detuning. For taps that are very close to the QPM wavelength, the required detuning becomes significant due to its hyperbolic dependence on $1/(\omega_{\mathrm{Di}} - \omega_{\mathrm{QPM}})$. It is worth noting that if the first tap is chosen reasonably far from the QPM wavelength., the phase tuning is limited to <20 GHz. However, the part of the spectrum that is close to the QPM wavelength could be wasted (i.e., fewer taps can be achieved). Furthermore, for delays that are

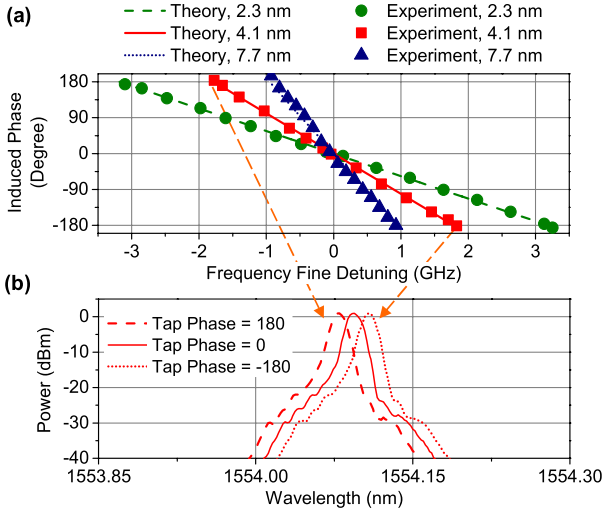

Fig. 4. (a) Measured phase induced by frequency fine-detuning for various tap-to-QPM wavelength distances. (b) Fine-detuning the wavelength of the dummy pump, λ_{D2}, which induces the phase delay in (a).

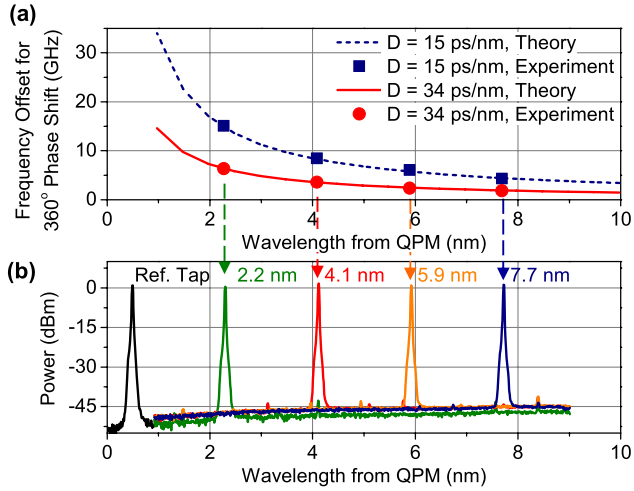

Fig. 5. (a) Required frequency detuning for 2π phase shift on a tap versus tap-to-QPM wavelength distance for various DCF lengths. (b) Spectrum showing tap delay variation.

very large, a very small amount of detuning might be required, which can be accomplished using acousto-optic modulators [12]. Utilization of external modulators for large numbers of taps can make the system more complex compared with the original LCoS approach. However, we note that if the taps' pump spacings are closer than the LCoS resolution, the pump fine frequency detuning approach might be preferred.

The effect of fine-detuning on time delay error is depicted in Fig. 6. According to Eqs. (4) and (5), the maximum relative delay error (corresponding to $\phi_i^{\mathrm{ADJ}} = \pm\pi$) decreases proportional to $\pi/(L\beta_2(\omega_{\mathrm{Di}} - \omega_{\mathrm{QPM}})(\omega_{\mathrm{Di}} - \omega_{D1}))$, i.e., higher tap delays experience lower delay errors, and larger dispersion values cause lower errors; therefore, we consider $D = 34$ ps/nm and the delay error is plotted versus a phase induced by the fine-detuning method. For our case, in which the signals are in the C-band, the worst case tap delay error is <10% and can be reduced by placing the taps farther from the QPM wavelength.

The amount of frequency fine-detuning required for a 2π phase shift depends on the distance to the tap from the QPM wavelength [Figs. 4(a) and 5(a)]. If longer DCFs are used, then finer tuning will be required. However, for a given tap delay (i.e., multiplication of DCF dispersion and wavelength separation is given), there is a trade-off between choosing longer DCFs and smaller wavelength spacing (i.e., more taps but shorter tap-delay tuning range) and shorter DCFs with a longer tap-tuning range. For both cases, the fine-detuning required can be made negligible compared with the tap-wavelength spacing. Because more taps (ω_{Di}) naturally appear further from the QPM wavelength and, consequently, the first tap, and because delay error is proportional to $1/((\omega_{\mathrm{Di}} - \omega_{\mathrm{QPM}})(\omega_{\mathrm{Di}} - \omega_{D1}))$, it is intrinsic to the scheme that when more taps are added, this delay error becomes negligible, as shown in Fig. 6.

To assess the effect of delay error on the output signal quality, a 31 Gbaud QPSK signal is sent to a 2-tap TDL with a one-symbol time delay between taps. As a result, the TDL works as a 2-tap QPSK correlator. Two taps are considered because they experience the largest delay

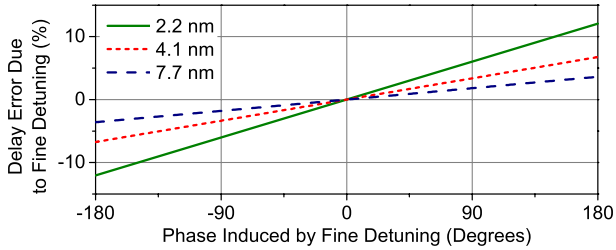

Fig. 6. Theoretical relative delay error versus phase applied by fine-detuning of pump wavelengths for $D = 34$ ps/nm dispersion at different delays (wavelength separation).

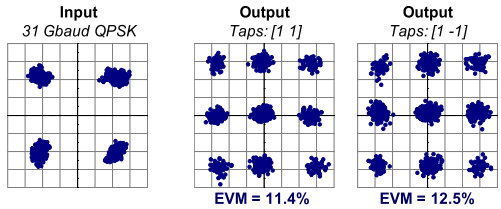

Fig. 7. Input 31-Gbaud QPSK signal constellation diagram and output of a 2-tap correlator with tap coefficients [1 1] and [1 −1].

error as a result of wavelength fine-detuning. Figure 7 depicts the input and output constellation diagrams, resulting in ~1% larger error vector magnitude (EVM) in the output signal when the tap phase is changed from 0 to π.

We acknowledge the support of DARPA under contracts FA8650-08-1-7820, N00014-05-1-0053 and W911NF-10-1-0151, NSF, and NSF CIAN.

References

1. J. G. Proakis, *Digital Communications* (McGraw-Hill, 2000).
2. S. Khaleghi, O. F. Yilmaz, M. R. Chitgarha, M. Tur, N. Ahmed, S. R. Nuccio, I. M. Fazal, X. Wu, M. W. Haney, C. Langrock, M. M. Fejer, and A. E. Willner, IEEE Photon. J. **4**, 1220 (2012).
3. B. Moslehi, J. W. Goodman, M. Tur, and H. J. Shaw, Proc. IEEE **72**, 909 (1984).
4. C. R. Doerr, S. Chandrasekhar, P. J. Winzer, A. R. Chraplyvy, A. H. Gnauck, L. W. Stulz, R. Pafchek, and E. Burrows, J. Lightwave Technol. **22**, 249 (2004).
5. M. S. Rasras, I. Kang, M. Dinu, J. Jaques, N. Dutta, A. Piccirilli, M. A. Cappuzzo, E. Y. Chen, L. T. Gomez, A. Wong-Foy, S. Cabot, G. S. Johnson, L. Buhl, and S. S. Patel, IEEE Photon. Technol. Lett. **20**, 694 (2008).
6. D. Hillerkuss, R. Schmogrow, T. Schellinger, M. Jordan, M. Winter, G. Huber, T. Vallaitis, R. Bonk, P. Kleinow, F. Frey, M. Roeger, S. Koenig, A. Ludwig, A. Marculescu, J. Li, M. Hoh, M. Dreschmann, J. Meyer, S. Ben Ezra, N. Narkiss, B. Nebendahl, F. Parmigiani, P. Petropoulos, B. Resan, A. Oehler, K. Weingarten, T. Ellermeyer, J. Lutz, M. Moeller, M. Huebner, J. Becker, C. Koos, W. Freude, and J. Leuthold, Nat. Photonics **5**, 364 (2011).
7. J. Capmany and D. Novak, Nat. Photonics **1**, 319 (2007).
8. S. Khaleghi, M. R. Chitgarha, O. F. Yilmaz, M. Tur, M. W. Haney, C. Langrock, M. M. Fejer, and A. E. Willner, *CLEO Conference* (2012), paper CM2B.4.
9. C. Langrock, S. Kumar, J. E. McGeehan, A. E. Willner, and M. M. Fejer, J. Lightwave Technol. **24**, 2579 (2006).
10. G. Agrawal, *Nonlinear Fiber Optics* (Academic, 2001).
11. Y. Dai, Y. Okawachi, A. C. Turner-Foster, M. Lipson, A. L. Gaeta, and C. Xu, Opt. Express **18**, 333 (2010).
12. S. R. Nuccio, O. F. Yilmaz, X. Wu, and A. E. Willner, Opt. Lett. **35**, 523 (2010).